Structured Kinetic Model to Represent the Utilization of Multiple Substrates in Complex Media During Rifamycin B Fermentation

Prashant M. Bapat, Sharad Bhartiya, K.V. Venkatesh, Pramod P. Wangikar

Department of Chemical Engineering, Indian Institute of Technology, Bombay, Powai, Mumbai 400 076, India; telephone: +91-22-2576 7232; fax: +91-22-2572 6895/2572 3480; e-mail: pramodw@iitb.ac.in

Received 5 April 2005; accepted 29 September 2005

Published online 21 November 2005 in Wiley InterScience (www.interscience.wiley.com). DOI: 10.1002/bit.20767

Abstract: Industrial fermentations typically use media that are balanced with multiple substitutable substrates including complex carbon and nitrogen source. Yet, much of the modeling effort to date has mainly focused on defined media. Here, we present a structured model that accounts for growth and product formation kinetics of rifamycin B fermentation in a multi-substrate complex medium. The phenomenological model considers the organism to be an optimal strategist with an in-built mechanism that regulates the sequential and simultaneous uptake of the substrate combinations. This regulatory process is modeled by assuming that the uptake of a substrate depends on the level of a key enzyme or a set of enzymes, which may be inducible. Further, the fraction of flux through a given metabolic branch is estimated using a simple multi-variable constrained optimization. The model has the typical form of Monod equation with terms incorporating multiple limiting substrates and substrate inhibition. Several batch runs were set up with varying initial substrate concentrations to estimate the kinetic parameters for the rifamycin overproducer strain *Amycolatopsis mediterranei* S699. Glucose and ammonium sulfate (AMS) demonstrated significant substrate inhibition toward growth as well as product formation. The model correctly predicts the experimentally observed regulated simultaneous uptake of the substitutable substrate combinations under different fermentation conditions. The modeling results may have applications in the optimization and control of rifamycin B fermentation while the modeling strategy presented here would be applicable to other industrially important fermentations.

Keywords: cybernetic models; substitutable substrates; amino acid uptake

INTRODUCTION

Optimization of a fermentation process is a key step in commercial production of antibiotics (Calam, 1987). This involves an optimization of the initial medium composition (Bapat et al., 2003; Bapat and Wangikar, 2004), optimal feeding strategy (ban Impe and Bastin, 1995) and better monitoring and control strategies (Komives and Parker, 2003). A large fraction of the commercially important antibiotics are produced by actinomycetes. The notable examples include penicillin, cephalosporins (Cohen et al., 1990), and erythromycin (Emblay, 1991). In fact, more than one thousand new secondary metabolites of actinomycetes are reported in the last 20 years alone (Euverink, 1995). Several of the industrial fermentations involving actinomycete species are carried out with complex media containing multiple substrates, some of which are derived from soybean, corn, barley, animal source, etc. (Calam, 1987). Despite the commercial importance of the actinomycetes in antibiotic production, there is a severe lack of mathematical models that accurately describe the growth and product formation in a complex media.

The growth in a multi-substrate, defined media has been studied for several species of bacteria. The growth pattern is classified into three broad categories: (i) sequential uptake of the substrates regardless of the pre-fermentor conditions, typically through catabolite repression (Doshi et al., 1997; Venkatesh et al., 1997). The pre-fermentor condition, or adaptation to a specific substrate, does not alter the sequence of substrate uptake. Examples include the sequence of uptake of sugars by *E. coli* K12 (Lendenmann and Egli, 1998), (ii) simultaneous uptake of substrates regardless of the pre-fermentor conditions. For example, the simultaneous uptake of glucose and organic acids by *E. coli* K12 is dependent on fermentor conditions but independent of pre-fermentor conditions (Venkatesh et al., 1997), (iii) substrate uptake pattern depending on pre-fermentor conditions or adaptation to specific substrates. Examples of this kind include uptake of phenanthrene by *Pseudomonas sp.strain PP* (Prabhu and Phale, 2003) and Benzyl alcohol utilization by *Pseudomonas putida* CSV86 (Basu et al., 2003).

The first structured dynamic model was proposed to account for the sequential uptake of substrates (Van Dedem

Correspondence to: P.P. Wangikar

Abbreviations used: CSL, corn steep liquor; Soya, defatted soybean flour; AMS, ammonium sulfate.

and Moo-Young, 1975). Structure to the model was added in the form of a key enzyme(s) that was assumed to control the substrate uptake. Likewise, the cybernetic perspective of microbial growth (Ramkrishna, 1982) assumes that the metabolic regulation of the growth processes is mediated through the control of enzyme synthesis and activity. The model assumes a priori that the enzyme for the preferred substrate is constitutive while that for the less preferred substrate is inducible by the substrates they act on. The enzyme synthesis is controlled by a cybernetic variable based on the matching law (Herrnstein, 1974), according to which the optimal allocation of resources towards the uptake of a substrate is proportional to the amount of returns obtained from that substrate. These models have been further refined to account for the sequential as well as simultaneous utilization of substrates (Doshi et al., 1997; Narang et al., 1997). For example, it was proposed that the growth process may be modeled with the help of a simple multi-variable constrained optimization, which aims at maximizing the specific growth rate (Doshi et al., 1997). The model assumes that the growth on a substrate is dependent on a control parameter, α, which is obtained dynamically by optimizing the specific growth rate under certain constraints. These and several other models assume the organism to be an optimal strategist, which chooses its substrate consumption pattern to maximize the chances of survival and propagation of its own species. The cybernetic models and the other related models have been successfully applied in predicting the growth and substrate uptake patterns of *E. coli* (Doshi et al., 1997; Doshi and Venkatesh, 1998; Lendenmann and Egli, 1998; Narang et al., 1997; Ramakrishna et al., 1997; Venkatesh et al., 1997), *Lactobacillus rhamnosus* (Bajpai-Dikshit et al., 2003), and *Chelatobacter heintzii* (Bally and Egli, 1996). The application of such models has been demonstrated for growth on defined media, which is substantially different from a complex media typically used in an industrial fermentation. Moreover, despite the industrial importance of the actinomycetes fermentation, only one report is available on structured model that describes the growth of *Streptomyces lividans* in a defined media (Daae and Ison, 1998).

Earlier, we have reported a strategy to design the optimum initial medium composition for batch fermentation (Bapat and Wangikar, 2004). Here we present a detailed dynamic model for the fermentation of rifamycin B, which is an antibiotic produced on industrial scale by genetically modified strains of *Amycolatopsis mediterranei*, an actinomycete, in a multi-substrate complex media (Richard and Lancini, 1975). The model considers the organism to be an optimal strategist and predicts the growth and product formation rates via a simple, multi-variable constrained optimization (Doshi et al., 1997). The kinetic model throws light on some interesting patterns of substrate inhibition towards growth and product formation. We address the following key questions related to the rifamycing B fermentation: (i) How to represent the kinetics of growth, product formation, and substrate utilization for the uptake of individual substrate combination? (ii) How to estimate the model parameters? (iii) How to mathematically represent the cellular regulatory processes underlying the sequence of substrate uptake? (iv) How to predict the substrate uptake sequence and the kinetics of growth and product formation in a multi-substrate complex medium? (v) What is the predictive value of such a model?

MATERIALS AND METHODS

Experimental Methods

Materials

The rifamycin B-producing strain, *A. mediterranei* S699, a gift from Professor Giancarlo Lancini at the former Lepetit Laboratories (Geranzano, Italy), was obtained from Prof. Heinz floss (Washington university, USA) (Yu et al., 2001). Rifamycin B standard was a gift from Lupin Pharma Ltd. (Mumbai, India). HPLC grade water was purchased from Merck (Mumbai, India). All other chemicals were purchased from Hi-Media (Mumbai, India) and General Foods (Indore, India).

Fermentation Protocol

The strain was cultivated and maintained as reported previously (Kim et al., 1996). The seed culture was prepared in medium containing 22 g/L glucose, 5 g/L meat extract, 5 g/L peptone, 5 g/L yeast extract, 3 g/L tryptone, and 1.5 g/L NaCl (Richard and Lancini, 1975). The fermentation media contained, per liter of distilled water, 1 g of potassium dihydrogen phosphate, 1 g of magnesium sulphate, 0.010 g of ferrous sulphate, 0.050 g of zinc sulphate, and 0.0030 g of cobalt chloride (Bapat and Wangikar, 2004). Additionally, the fermentation media was supplemented with specified quantities of glucose, ammonium sulfate (AMS), Soya flour, and corn steep liquor (CSL). Fermentation was initiated by inoculating the fermentation medium with 10% v/v seed culture. All the fermentation experiments were performed in triplicate.

Analytical Techniques

Samples were drawn from the fermentation medium at regular intervals to analyze the dry cell weight and the concentrations of glucose, AMS, free amino acids, and rifamycin B. Dry cell weight was measured by first removing the insoluble substrates, which settle under gravity and then by filtering the supernatant with a pre-weighed (Type 1 Whatmann filter paper, Whatmann, Inc., Brentford, Middlesex, UK) filter paper (Gygax et al., 1982). Glucose was analyzed via RI detector in HPLC (Hitachi, Merck KgaA, Darmstadt, Germany) using HP-Aminex-87-H column (Biorad, Inc., Hercules, CA) at 60°C with a mobile phase of 5 mM sulfuric acid, flow rate was kept at 0.6 mL per minute. Rifamycin B was detected on spectrophotometer (V-540, Jasco, Tokyo, Japan) at a wavelength of 425 nm as

described (Pasqualucci et al., 1970). AMS was measured using ion analyzer (EA940 Ion analyzer, Thermo Orion, Beverly, MA). The concentration of free amino acids was estimated via the ninhydrin method (Moore, 1968). Four mililiter of sample, upon appropriate dilution, was mixed with 1 mL of the ninhydrin reagent containing 3 g/L of hydrindantin and 20 g/L ninhydrin. The mixture was boiled for 15 min, and then cooled to room temperature and the absorbance at 575 nm was measured on spectrophotometer (V-540, Jasco) to obtain the concentration of free amino acids.

Model Development and Parameter Estimation

The model formulation and parameter estimation was achieved in two stages: (i) an unstructured model was developed that explains the growth and product formation in the presence of substrates that are simultaneously taken up without any apparent regulation. The model parameters were estimated via experiments involving individual substrate combinations; (ii) structure was added to the model to account for regulated sequential/simultaneous uptake of substrates in a multi-substrate environment. We describe these two stages in detail below.

Unstructured Model for Growth on Two Substrates

As our preliminary results (Bapat and Wangikar, 2004) had indicated an optimum substrate concentration for growth and product formation, the cell growth rate was modeled by using Monod equation, which incorporates terms for multiple limiting substrates with substrate inhibition terms (Equation (1)) (Birol et al., 2001). Since we use two limiting substrates in the medium, the Monod equation represented here is a product of two substrate terms. It may be noted that these two substrates, S_i and S_j are mutually non-substitutable. The substrate inhibition terms in Equations (1) and (2) can potentially account for the lower growth and product formation rates observed at higher substrate concentrations. Although the fermentation medium was composed of nine different components, we used only two of the nutrients in the model as some of the micronutrients such as potassium dihydrogen phosphate, manganese sulphate, ferrous sulphate, cobalt chloride, and zinc sulphate did not affect the growth and productivity significantly as long as the concentrations of these micronutrients were within the predetermined range (Bapat and Wangikar, 2004). The specific growth rate (μ_k) and specific product formation rate ($q_{\mathrm{p},k}$) on a substrate combination k, made up of substrates S_i and S_j are given by Equations (1) and (2), respectively.

$$\mu_k = \frac{1}{X}\frac{\mathrm{d}x}{\mathrm{d}t} = \mu_k^{\max}\frac{S_i}{K_{s_i}+S_i+\frac{S_i^2}{K_{I,i}}}\frac{S_j}{K_{s_j}+S_j+\frac{S_j^2}{K_{I,j}}} \tag{1}$$

$$q_{p,k} = \frac{1}{X}\frac{\mathrm{d}p}{\mathrm{d}t} = q_{p,k}^{\max}\frac{S_i}{K_{\mathrm{p}_i}+S_i+\frac{S_i^2}{K_{P_{I,i}}}\frac{S_j}{K_{\mathrm{p}_j}+S_j+\frac{S_j^2}{K_{P_{I,j}}}}} \tag{2}$$

The model parameters such as $\mu_k^{\max}$, $q_{\mathrm{p},k}^{\max}$, K_S, K^{P}, K_I, and $K^{\mathrm{P},I}$ for each substrate combination S_i and S_j were estimated in a two-step process. First, a rough estimate of these parameters was obtained by measuring the initial growth and product formation rates at different initial concentrations of one substrate while maintaining a constant concentration of the other substrate. These estimates were further fine-tuned by fitting the dynamic Equations (1) and (2) to the time profiles of the batch data. This was achieved by employing the dynamic optimization algorithm ''fmincon'' available in the software MATLAB (Mathworks, Natick, MA). The following objective functions (Equations (3) and (4)) were optimized while fine-tuning the model parameters.

$$\phi_x = \sum_o \left(X_i^{\exp} - X_i^{\mathrm{calc}}\right)^2 + \sum_i \left(S_i^{\exp} - S_i^{\mathrm{calc}}\right)^2 \tag{3}$$

$$\phi_p = \sum_i \left(X_i^{\exp} - X_i^{\mathrm{calc}}\right)^2 + \sum_i \left(S_i^{\exp} - S_i^{\mathrm{calc}}\right)^2 + \sum_i \left(P_i^{\exp} - P_i^{\mathrm{calc}}\right)^2 \tag{4}$$

Where ϕ_x and ϕ_p represents parameter optimization criteria for biomass and product formation, respectively. X_i, S_i, and P_i represent biomass, substrate concentration, and rifamycin B concentration, respectively.

Structured Model for Growth in a Multi-Substrate Environment

The complex medium contain soluble and insoluble portion of Soya flour and CSL with glucose and AMS. The model assumes that the organism has access to upto three substrate combinations in this complex medium (Fig. 1). The three combinations are: (i) soluble portion of Soya flour and CSL, typically available as free amino acids (S_1); (ii) S_1 and glucose (S_2); (iii) S_2 and AMS (S_3). The insoluble portion of Soya flour and CSL (S_4) first needs to be solubilized to S_1, which can then be taken up in combination (i) or (ii) above. The specific growth rate (r_k) and the specific product formation rate ($q_{\mathrm{P},k}$) are defined on each substrate combination independently by Equations (5) and (6), respectively. This kinetic form has an additional term for the key enzyme, $e_k/e_k^{\max}$ involved in the uptake of a specific substrate combination.

$$r_k = \mu_k \frac{e_k}{e_k^{\max}} \tag{5}$$

$$q_{\mathrm{P},k} = q_{\mathrm{P},k}\frac{e_k}{e_k^{\max}} \tag{6}$$

Where μ_{k} and $q_{\mathrm{P},k}$ are given by Equations (1) and (2), respectively. The flux flowing towards cell growth through a specific branch (substrate combination) is regulated via the control of the metabolic network (Fig. 1). The control may

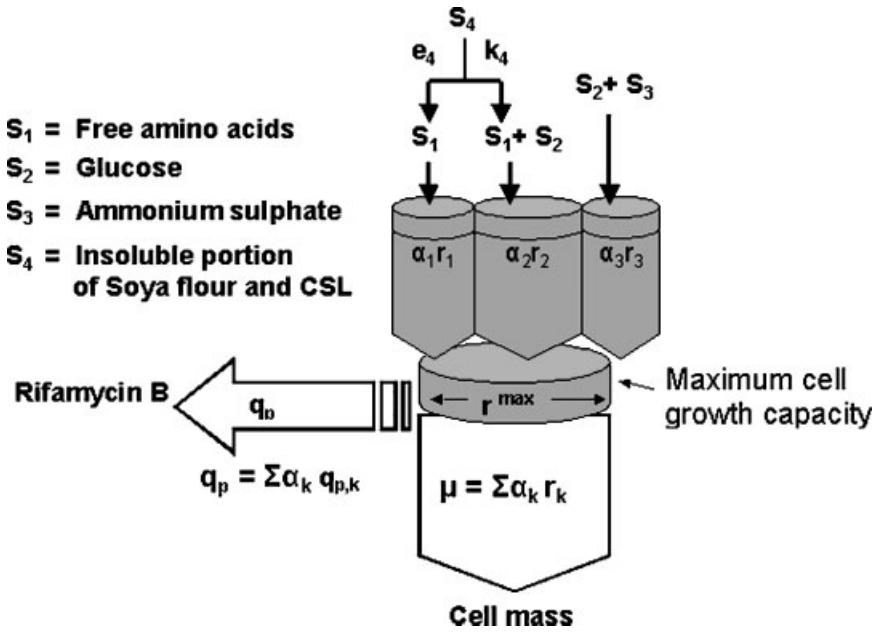

Figure 1. Schematic for the structured model to represent growth, product formation, and substrate utilization by *Amycolatopsis mediterranei* S699 in a complex media containing multiple substrates. The model assumes that the organism has access to upto three substrate combinations for growth. Free amino acids are made available via enzymatic hydrolysis (e_4) of peptides/proteins in Soya-CSL (S_4). The specific growth rate (r_k) and the specific product formation rate ($q_{P,k}$) are defined on each substrate combination independently. The flux through a given branch (α_k) is obtained via a multiconstraint optimization (Venkatesh et al., 1997). The figure concept from Nielsen and Villadsen (1994).

be complex in its mechanism involving several genes and enzymes. We model this metabolic control phenomenologically via a control parameter, α_k, as the fraction of flux toward growth from the kth substrate combination (Doshi et al., 1997). Thus, the overall specific growth rate, μ, is a sum of the fraction of specific growth rates on the individual substrate combinations and is given by Equation (7). Likewise, the overall specific product formation rate is given by Equation (8), which assumes that the control parameters, α_k's, which determine the fraction of flux through a branch toward growth also determine the fraction of flux toward product formation. Since the key enzymes captures the metabolic state of the cell, it is reasonable to assume that the values of the control coefficients for growth and product formation for a given substrate combination is the same.

$$\mu = \sum_{k=1}^{3} \alpha_k r_k \tag{7}$$

$$q_P = \sum_{k=1}^{3} \alpha_k q_{P,k} \tag{8}$$

The non-dimensional term for the key enzyme ($e_k/e_k^{\max}$) can vary between 0 and 1.0 and can potentially be regulated by transcriptional, translational or other regulatory mechanisms. The specific key enzyme synthesis rate is formulated as described by Kompala et al. (1984) and is assumed to be proportional to the control parameter, α_k, which controls the flux in that particular branch. The rate of change of the non-dimensionalized values of key enzyme $e_k/e_k^{\max}$ corresponding to the uptake of kth substrate is given by Equation (9) (Doshi et al., 1997).

$$\frac{\mathrm{d}(e_k/e_k^{\max})}{\mathrm{d}t} = \alpha_k(\mu_k^{\max} + \beta_k) \left[\frac{S_i}{(K_{s_i} + S_i + \frac{S_i^2}{K_{I,i}})} \times \frac{S_j}{(K_{s_j} + S_j + \frac{S_j^2}{K_{I,j}})}\right] - (\mu + \beta_k)\frac{e_k}{e_k^{\max}} \tag{9}$$

Where the parameter β_k represents the first order degradation rate constant for the key enzyme. It is known that the uptake of amino acids is repressed by the presence of other carbon sources (Benko et al., 1969). Thus, the rate of synthesis of e_1 was assumed to be inhibited by the presence of glucose as given in Equation (10).

$$\frac{\mathrm{d}(e_k/e_k^{\max})}{\mathrm{d}t} = \alpha_1(\mu_1^{\max} + \beta_1) \left[\frac{s_1}{(K_{s_1} + S_1 + \frac{S_1^2}{K_{I,1}} + S_2)}\right] - (\mu + \beta_1)\frac{e_1}{e_1^{\max}} \tag{10}$$

The rate of substrate uptake can be related to the rate of growth and product formation via yield coefficients for cell mass (Y_{X/S_i}) and product (Y_{P/S_i}) on the substrate S_i (Equation (11)).

$$\frac{\mathrm{d}S_i}{\mathrm{d}t} = -\sum_{k=1}^{3} \alpha_k \left[\frac{1}{Y_{X/S_i}} r_k + \frac{1}{Y_{P/S_i}} q_{P,k}\right] X \tag{11}$$

The mass balance for free amino acids (S_1) involves an additional term for the zeroth order solubilization of the insoluble portion of Soya flour and CSL (S_4) via an enzymatic process involving a solubilizing enzyme e_4 with a rate constant k_4 (Equation (12)). We assume that the enzyme e_4 is induced when the total soluble nitrogen (N_T), present in the form of S_1 and S_3, starts depleting (Equation (13)).

$$\frac{dS_1}{dt} = -\sum_{k=1}^{3} \alpha_k \left[\frac{1}{Y_{X/S_i}} r_k + \frac{1}{Y_{P/S_i}} q_{P,k} \right] X + k_4 \frac{e_4}{e_4^{max}} X \quad (12)$$

$$\frac{d(e_4/e_4^{max})}{dt} = \frac{(\mu + \beta_4)}{1 + (N_T/K)^n} - (\mu + \beta_4) \frac{e_4}{e_4^{max}} \quad (13)$$

The fraction α_k's are estimated using the optimality criteria (Doshi et al., 1997). The organism allows the uptake of all the substrate combinations as long as the specific growth rate obtained by summing the rates on different substrates (Equation (7)) is less than the intrinsic growth capacity (μ_{max}). Under the conditions where the sum of the specific growth rates exceeds μ_{max}, the control parameters are set to prefer the uptake of the substrate that offers highest growth rate. This is mathematically shown in Equation (14).

$$\begin{aligned} &\max(\mu), \\ &\text{s.t.}\{,\ 0 \le \alpha_k \le 1, \\ &\text{and } \mu \le \mu_{max} \end{aligned} \quad (14)$$

Simulation of the Growth and Product Formation Profiles

The simulation exercise to predict the cell growth, product formation, and substrate utilization was carried out by solving the set of simultaneous differential equations (Equations 5–14) as an initial value problem. The initial values were specified in the form of initial media compositions and the initial values of the enzyme levels (e_k/e_k^{max}). The simulations were performed using the ODE45 solver available with the Matlab software (Mathworks).

RESULTS

Previously, we have reported an optimized initial medium composition for rifamycin B fermentation in shake flasks (Bapat and Wangikar, 2004). This was achieved by a guided search method to explore the vast search space of all the different media compositions. In the process, we had conducted batch runs of over 140 different medium compositions and observed that the final cell mass and product concentrations were highly sensitive to the medium components such as glucose, AMS, and Soya flour (data not shown). With these preliminary results, here we have carried out further kinetic analysis of the growth, product formation, and substrate utilization based on the major nutrients such as glucose, AMS, and mixture of defatted soybean flour (Soya) and CSL. The kinetic analysis was performed with a rifamycin B overproducer strain, *Amycolatopsis mediterranei* S699, that does not require barbital (Yu et al., 2001).

Parameters for the Unstructured Model

From the substrates listed above, we have chosen medium compositions comprising substrates that are mutually non-substituting. These media combinations include: (i) soluble portion of Soya-CSL; (ii) glucose and Soya-CSL; and (iii) glucose and AMS. In each of the medium compositions, the substrates were taken up simultaneously without any apparent regulation. An unstructured model, as represented by Equations (1) and (2), was found to be adequate in such situations.

The model parameters were estimated by fitting the model to the experimental data using fmincon program of Matlab. Model fit was obtained for the duration excluding the lag phase. A total of 19 batches were set up with varying initial concentrations of the nutrients. Specifically, the initial concentrations of glucose, AMS, and mixture of Soya-CSL were varied in the range of 0–190, 0–12.5, and 0–120 g/L, respectively. In the first set of experiments, growth was monitored on two different initial concentrations of the Soya-CSL. Insoluble portion of the Soya-CSL was omitted from the medium to facilitate accurate monitoring of the nutrient-consumption and cell growth. The soluble portion of the Soya-CSL mainly contained free amino acids. Depletion of amino acids was concomitant with the cell growth (Fig. 2), but the growth ceased after reaching a dry cell weight of around 2.0 g/L despite the availability of free amino acids. This is possibly due to the unfavorable C/N ratio of amino acids with excess nitrogen than that required for growth. No product formation was observed during growth on Soya-CSL alone. The model fits well with the experimental data for the first 40 h of growth. These batches were characterized by a strong ammonia smell toward the end of the logarithmic growth phase.

In a second set of experiments, six batches were set up with a fixed initial concentration of glucose and varying initial concentration of the Soya-CSL. AMS was not used in the media in this batch of experiments. Two representative batches are shown in Figure 3 demonstrate the overall trend observed when grown on combination II. The final biomass and rifamycin B concentrations were in the range of 8.20–24.0 g/L and 1.60–3.20 g/L, respectively. In these batches, glucose plays the role of carbon-source while the free amino acids available from the Soya-CSL play the role of nitrogen source. The model fits well with the experimental data for these sets of experiments (Fig. 3). Towards the end of the batch, the experimentally observed uptake rate of glucose was lower than that predicted by the model. This could potentially be due to the slow process of solubilization of the insoluble portion of the Soya flour and CSL which would limit the availability of free amino acids and in turn the growth rate.

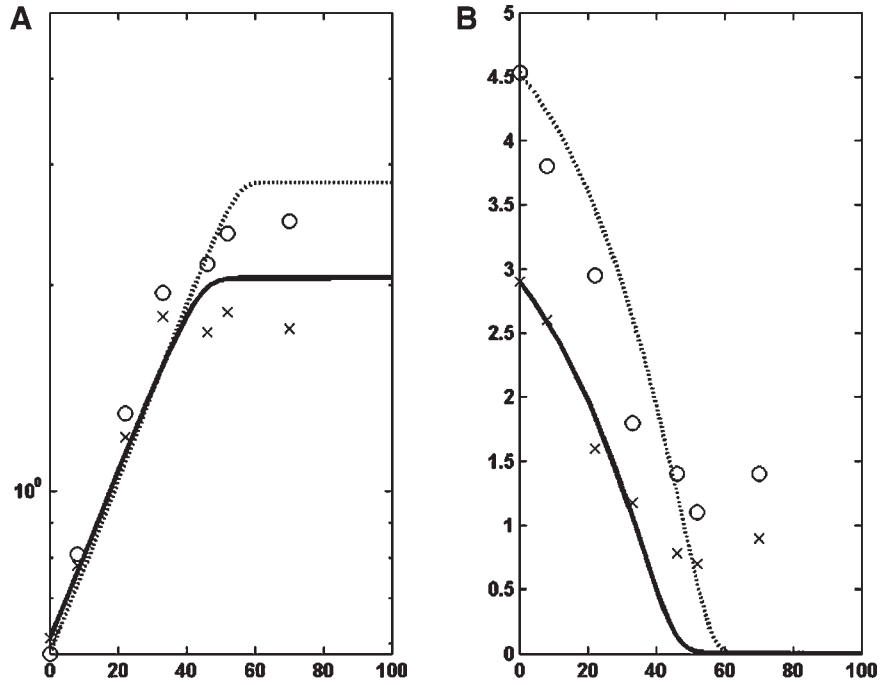

Figure 2. Growth of *A. mediterreniae* S699 on amino acids alone (i.e., substrate combination I. The initial concentration of free amino acids was obtained by dissolving different quantities of Soya-CSL in water. Additionally, the media contained micronutrients 11 g/L $CaCO_3$, 1 g/L KH_2PO_4, 1 g/L $MgSO_4$, 0.01 g/L $FeSO_4$, 0.05 g/L $ZnSO_4$, 0.003 g/L $CoCl_2$. initial Soya-CSL: 40 g/L; ○ initial Soya-CSL; 80 g/L. **A**: Dry cell weight (g/L); (**B**) free amino acid concentration (g/L). Lines represent simulation results using the unstructured model.

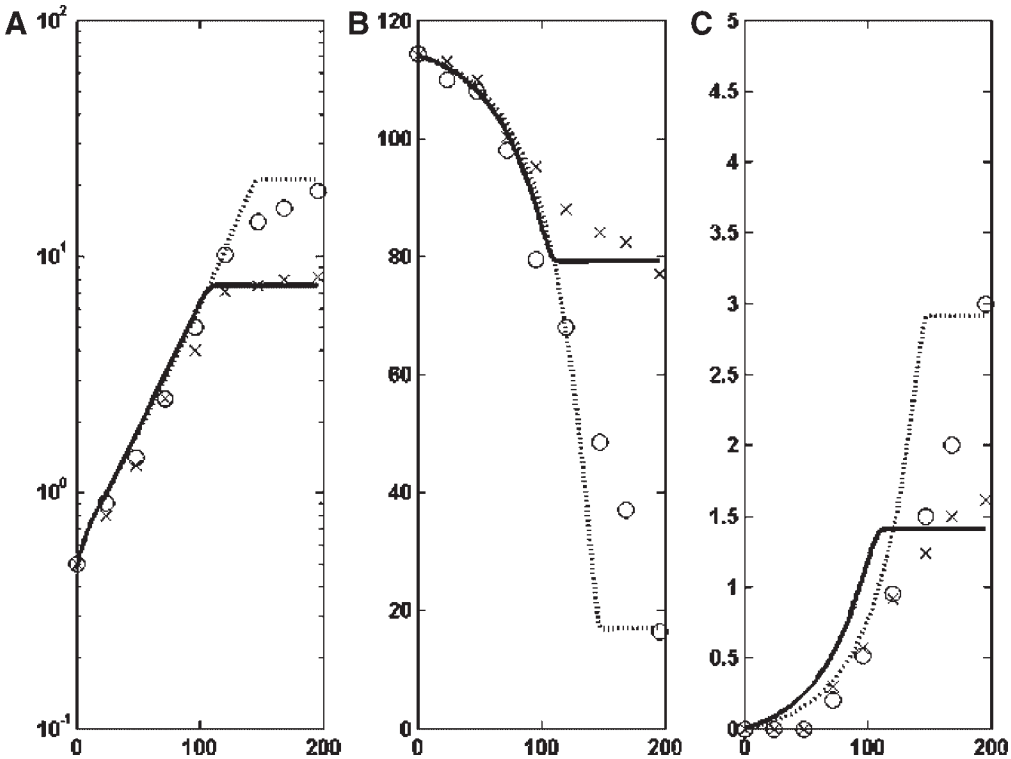

Figure 3. Profile for growth on glucose and Soya-CSL (i.e., substrate combination II. Both soluble and insoluble portions of Soya-CSL were used. The medium contained 120 g/L glucose and the micronutrients as shown in legend to Figure 2. : initial Soya-CSL: 20 g/L; ○ initial Soya-CSL; 30 g/L. **A**: Dry cell weight (g/L); (**B**) glucose concentration (g/L); (**C**) rifamycin B concentration (g/L). Lines represent simulation results using the unstructured model.

Six batches were set up with varying initial concentration of glucose and fixed initial concentration of AMS. Five batches were set up with varying initial concentration of AMS and fixed initial concentration of glucose. In these two sets of experiments, complex source was not used in the media. The cell growth profile was concomitant with the glucose and AMS uptake profiles. Experimental data along with model fit has been shown for representative batches (Fig. 4). The growth profiles were marked by a lag phase, an exponential growth phase followed by a slower exponential growth phase (Fig. 4A). The model simulation results are shown from the end of the lag phase; 47 and 59 h for the batches containing 80 and 120 g/L glucose, respectively. The lag phase increased with increasing initial AMS and glucose concentrations (data not shown). These trends point toward the potential substrate inhibition for growth and product formation. A dominant substrate inhibition effect is apparent for AMS followed by that for glucose.

The experimentally estimated values of the model parameters are listed in Table I. For growth on Soya-CSL alone, the specific growth rates were much lower than those on the other two medium compositions. This can possibly result due to the fact that Soya-CSL alone is not a balanced medium from the point of view of C/N ratio in the medium. With substrate combination II, where Soya-CSL is balanced with dextrose, relatively higher specific growth rates are observed with moderate product formation rates. In medium composition II and III, Glucose is the common substrate while the nitrogen source is different. Interestingly, the model parameters relating to glucose are comparable to each other in these two types of medium compositions. This includes the cell mass yield on Glu ($Y_{x/s}$), half saturation constant for growth on Glu (K_s), inhibition constant on Glu (K_i), and half saturation constant for product formation on Glu (K_p). Of the three medium compositions, the highest value of μ_{max} was observed for growth on glucose and AMS. While no product formation was observed on medium containing soluble portion of soy flour and CSL (composition I), the maximum specific product formation rates (q_p^{max}) are comparable on medium compositions containing glucose and AMS (composition II) and glucose and Soya-CSL (composition III). However, on the defined medium composition II, a severe substrate inhibition is observed for growth and product formation with AMS. This type of severe substrate inhibition is not observed with the complex insoluble nitrogen source present in medium composition II. Thus, although the observed rates of growth were marginally higher on defined medium composition than those on complex medium, the observed product formation rates were comparable.

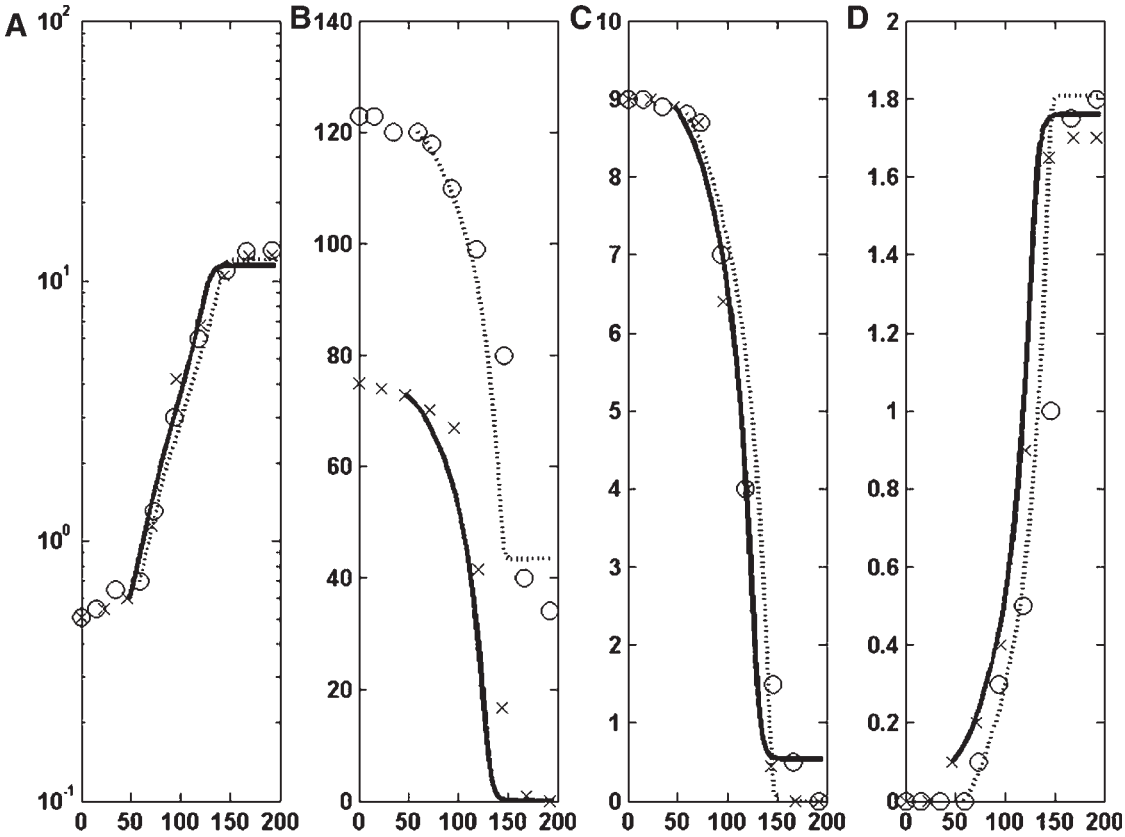

Figure 4. Profile for growth on glucose and AMS (i.e., substrate combination III. The initial medium composition contained 9.0 g/L $(NH_4)_2SO_4$, and the micronutrients as shown in legend to Figure 2. : initial glucose: 75 g/L; ○ initial glucose: 123 g/L. **A**: Dry cell weight (g/L); (**B**) glucose concentration (g/L); (**C**) AMS concentration (g/L); (**D**) rifamycin B concentration (g/L). Lines represent simulation results using the unstructured model.

Table I. Model parameters for growth and product formation in rifamycin B fermentation using the strain *Amycolatopsis mediterranei* S699[a].

Media composition	Growth parameters							Product formation parameters						
	μ_{max} (per h)	K_{s_i} (g/L)	K_{s_j} (g/L)	$K_{I,i}$ (g/L)	$K_{I,j}$ (g/L)	Y_{X/S_i} (g/g)	Y_{X/S_j} (g/g)	q_p^{max} (per h)	K_{p_i} (g/L)	K_{p_j} (g/L)	$K_{p_{I,i}}$ (g/L)	$K_{p_{I,j}}$ (g/L)	Y_{P/X_i} (g/g)	Y_{P/X_j} (g/g)
Composition I: Soya flour and corn steep liquor (S_i)	0.030	0.30	—	—	—	0.41	—		—	—	—	—	—	—
Composition II: glucose (S_i) and Soya flour and corn steep liquor (S_j)	0.075	25	0.45	100	125	0.40	1.70	0.019	25	0.45	80	125	0.30	1.7
Composition III: glucose (S_i) + ammonium sulphate (S_j)	0.155	15	1.40	100	4.50	0.19	1.70	0.0205	15	1.0	100	4.50	0.107	0.85

[a]The parameters were estimated by fitting the dynamic, growth Equation (1) and product formation Equation (2) to the various batches shown in Figures 1–4.

$$\frac{1}{X}\frac{dx}{dt} = \mu^{max}\frac{S_i}{K_{s_i}+S_i+\frac{S_i^2}{K_{I,i}}}\frac{S_j}{K_{s_j}+S_j+\frac{S_j^2}{K_{I,j}}} \quad (1)$$

$$\frac{1}{X}\frac{dp}{dt} = q_p^{max}\frac{S_i}{K_{p_i}+S_i+\frac{S_i^2}{K_{p_{I,i}}}}\frac{S_j}{K_{p_j}+S_j+\frac{S_j^2}{K_{p_{I,j}}}} \quad (2)$$

Structured Model Predictions

Validation With Individual Substrate Combinations and Setting the Initial Conditions

The Equations 5–14, which represent the structured model, were solved simultaneously for individual combinations of substrates to validate the parameters obtained in Section 3.1 above (Table I). The structured model was able to accurately predict the lag, growth, and product formation kinetics on individual substrate combinations (results not shown). Specifically, the unstructured model was able to fit the data from the time point in the batch where exponential growth phase begins (Figs. 2 and 3). On the other hand, the structured model is able to fit the data including the lag phase (simulation results not shown). As the seed culture was grown on a medium containing mainly free amino acids, we assume that the enzyme for the uptake of amino acids is in induced state at the beginning of the batch, while the other two enzymes are at basel level. Based on this criteria, the initial values of the key enzymes (e_k/e_k^{max}) were adjusted to fit the batch data for the individual substrate combinations. Thus, the initial values for e_1/e_1^{max}, e_2/e_2^{max}, and e_3/e_3^{max} were set to 0.95, 0.005, and 0.005, respectively (Table II). Likewise, the initial value of the solubilizing enzyme e_4 was set to a basal level of 0.005. The dissolution rate constant k_4 was estimated by assuming a pseudo-steady state level for soluble amino acids (Table II). The model accounts for the lag in growth and product formation by virtue of a delay in the induction of the key enzymes. For example, growth on glucose and AMS shows a longer lag phase than that on glucose and Soya flour and CSL (results not shown). This was captured in the delay in the induction of the enzyme e_3 that plays a key role in the uptake of glucose and AMS. Likewise, satisfactory fit was obtained in other batches.

Validation on Multi-substrate Complex Media

The structured model with the parameters (Table I) and initial conditions (Table II) obtained from the individual substrate combinations was used to predict a priori the growth, product formation, and substrate utilization in a complex media containing all the three substrate combinations. Batch runs were carried out with complex media to verify the model predictions for media containing 120 g/L glucose, 7 g/L

Table II. Model parameters used in simulating the batch fermentation profile.

Parameters	Parameter value
Initial enzyme levels	
e_1/e_1^{max}	0.95
e_2/e_2^{max}	0.005
e_3/e_3^{max}	0.005
e_4/e_4^{max}	0.005
Enzyme degradation constants	
$\beta_1=\beta_2=\beta_3=\beta_4$	0.004/h
Dissolution rate constant (k_4)	0.01/h

AMS, 8 g/L Soya flour, and 32 g/L of CSL. Figure 5 shows the comparison of experimentally observed profiles of cell density, rifamycin B, glucose, AMS, and amino acids with the model predictions. The model was able to accurately predict the growth, product formation, and substrate uptake (Fig. 5A). The highest deviation from predicted values was observed for AMS with the model predicting a delay of ca. 8 h compared with the experimental observations (Fig. 5C).

The biomass profile for the growth on complex medium is shown in Figure 5A. The overall biomass profile shows two distinct phases of growth; the first phase with a specific growth rate of 0.04/h between 0 and 110 h and the second phase with a growth rate of 0.01/h between 110 h to end of the fermentation. A similar profile can also be observed for the glucose uptake (Fig. 5B). In case of nitrogen (Fig. 5C), initially the free amino acids are utilized mainly for growth in the first 35 h and later the ammonium sulphate is the main nitrogen source between 40 and 120 h. The insoluble nitrogen is taken up only after the exhaustion of ammonium sulphate and free amino acids present in the medium. In this phase, the solublizing enzyme e_4 determines the availability of amino acids and in turn the growth rate. Therefore, the above three phases of uptake of nitrogen will determine the overall growth and product formation. The product formation begins at 50 h and is concominant with the onset of AMS uptake. The second phase of product formation begins at 120 h, which coincides with the exhaustion of AMS. In this phase, the product formation is on glucose and amino acids drawn from insoluble pool of the media. The optimal model is able to capture the above observed phase of growth and product formation. This can be clearly visualized by the profile of key enzymes (Fig. 5E), the control parameters (Fig. 5F), the specific growth rates (Fig. 5G), and the specific product formation rate (Fig. 5H). The enzyme e_1 is in the induced state while enzymes e_2 and e_3 are at basal levels of expression at the beginning of the batch due to the pre-culturing conditions. Since the sum of the growth rates due to the three substrate combination is less than maximum growth capacity of the cell (μ_{max}), e_2 and e_3 are induced to facilitate the uptake via r_2 and r_3. The level of e_1 decreases due to glucose repression in the uptake of amino acids.

The model is able to capture the metabolic state based on the uptake of different individual combinations. For example, as seen in Figures 5E and G, the contributions of different combinations of substrates to the overall growth rate can be predicted using the model. The initial growth rate is dominated by growth on free amino acids present in a media, which acts as both carbon and nitrogen source. Since e_2 and e_3 are induced during this phase, r_2 and r_3 can now contribute simultaneously to the growth rate. The growth rate obtained in this phase from r_2 and r_3 is less than the maximum capacity

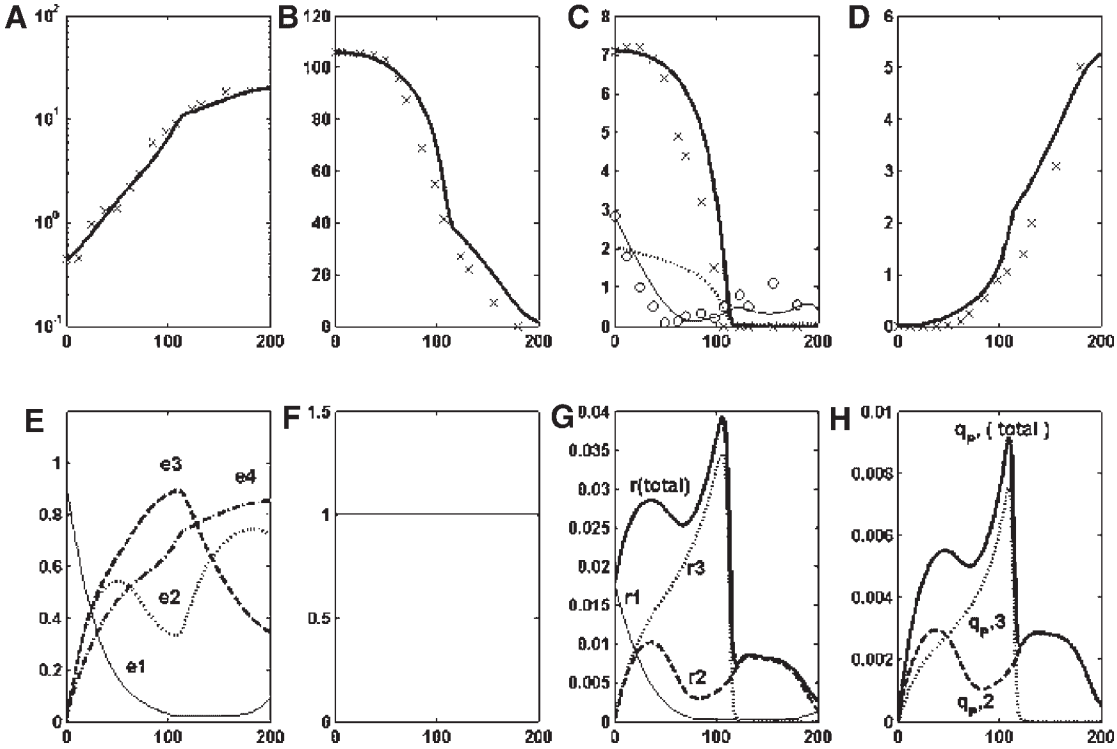

Figure 5. Structured model predictions for growth in a multisubstrate environment. Model predictions using structured model (shown as lines) are compared to the experimental data. The initial medium contained 120 g/L glucose, 7 g/L AMS, 8 g/L Soya flour, and 32 g/L of CSL and other micronutrients as shown in legend to Figure 2). **A**: Dry cell weight (g/L); (**B**) glucose concentration (g/L); (**C**) nitrogen source concentration (g/L) (: AMS, o: free amino acids, dotted line represent simulated total nitrogen N_T); (**D**) rifamycin B concentration (g/L); (**E**) simulated profiles of key enzymes required for the substrate uptake; (**F**) simulated profile of the control coefficients α_k; (**G**) simulated profiles of the specific growth rates r_k on the three media combinations; (**H**) simulated profiles of the specific production rates $q_{p,k}$ on the three media combinations.

of the cells, which is reflected in $\alpha_1 = \alpha_2 = \alpha_3 = 1$. The growth rate r_2 decreases around 70 h due to limiting amino acids concentration, although glucose is available as the carbon source. The glucose and AMS contribute towards the growth rate by r_3, which dominates in this phase of growth. The growth rate based on r_3 decreases sharply due to exhaustion of in ammonium sulphate around 110 h. The last phase is dominated by growth on amino acids and glucose (i.e., r_2), but the amino acids contribution is dependent on the rate of solublization of insoluble nitrogen in the complex media.

Similarly, the model is also able to capture the product formation rates in complex media. The maximum product formation rate is observed on glucose and AMS around 110 h ($q_{p,3}$), but the net productivity is greater on glucose and amino acids ($q_{p,2}$) (Fig. 5H). This can be seen by the area under the two curves represented by $q_{p,2}$ and $q_{p,3}$. As in the case of growth, the final phase of product formation beyond 120 h also dependent on the rate of solublization of amino acids for insoluble portion of complex medium.

The model was also used to predict another medium condition consisting of 80 g/L glucose, 3.9 g/L ammonium sulphate, 8 g/L Soya flour, and 32 g/L CSL (Fig. 6). This batch contained lower amounts of ammonium sulphate and glucose than the previous one. Although the final biomass and product concentrations are same as observed before, the rates are greater and reach the maximum value earlier than the previous result. For example, the AMS is completely consumed around 75 h in this batch as compared to 110 h in the previous batch (Figs. 5C and 6C). Moreover, the productivity of rifamycin B increases from 0.025 to 0.03 g/L/h (refer Figs. 5H and 6H).

The model is thus able to compare the variations in the metabolic state caused due to changes in the media composition. For example, due to the lower AMS concentration, the key enzyme e_3 is induced earlier (Fig. 6E) and this reflects in higher growth rate as well as productivity. The control parameter α_k clearly shows that for this combination of substrate concentrations, the cells reach the maximum growth capacity (μ_{max}) of 0.04/h around 30 h (Figs. 6F and G). Further, this maximum growth rate is sustained for about 40 h. It is seen from the Figure 6F that in this period, the growth on substrate combination I (i.e., amino acids alone) is curtailed in favor of growth on the other two combinations. Furthermore, r_2 is also partially curtailed in this period, during which the maximum growth rate is achieved mainly on substrate combination III. It can be noted that no such shift in the metabolic state was observed when higher amounts of glucose and ammonium sulphate was used (Fig. 5F). Figure 6H shows the overall product formation rate which is higher by 1.5 times than the previous example. The model developed here is thus able to capture the changes in the rate profile due to lower inhibition caused by ammonium sulphate.

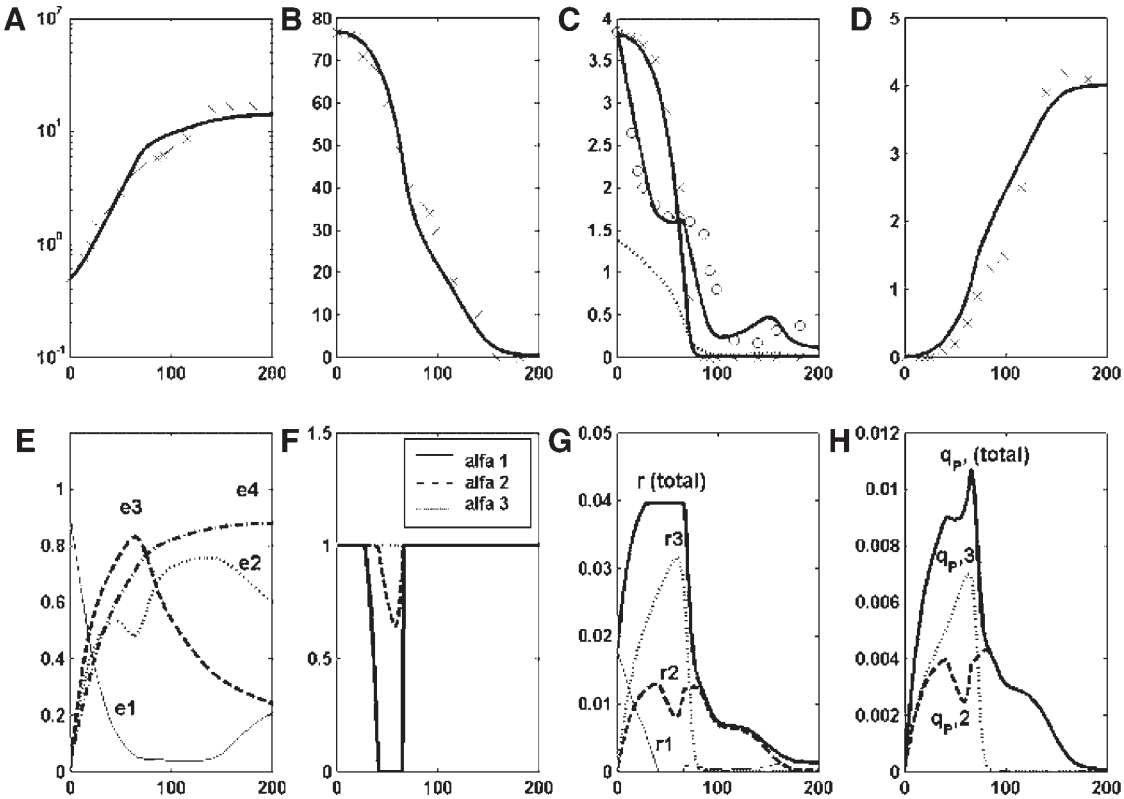

Figure 6. Structured model predictions for growth in a multisubstrate environment for a different initial medium composition compared to Figure 5. The initial medium contained 80 g/L glucose, 3.9 g/L AMS, 8 g/L Soya, and 32 g/L of CSL and other micronutrients as shown in legend to Figure 2. Lines represent simulation results. Legends to Figure 6A–I are same as the respective panels in Figure 5A–I.

DISCUSSION

Modeling of growth and product formation on complex media containing multiple substituable substrates is a challenge. Complex media offers the organism multiple choices of carbon and nitrogen substrate combinations. These include free amino acids, peptides, soluble, and insoluble proteins in addition to a defined carbon and nitrogen sources, such as glucose and ammonium sulphate. Kinetic models have not been formulated by incorporating these components of complex media. This makes the prediction of growth and product formation on complex media difficult.

Modeling strategies to predict growth and product formation on complex media are essential for various industrial applications. For example, a predictive model can be used to optimize a fed-batch strategy. The model can also be used to obtain inferential measurement and better control with fault diagnosis in a batch or a fed-batch process. Complex media are also prone to batch to batch variations in compositions. This can in turn lead to variability in productivity. A model can be utilized to take corrective measures to offset the adverse effects due to this variability.

Here, we have presented a model to predict the growth of *A. mediterranei* S699 on a complex media. A two stage modeling strategy was employed. An unstructured model was used to first estimate the Monod parameters. The unstructured model explains the observed trends very well when the substrates are co-utilized without any apparent regulation. However, the unstructured model could not explain the patterns of growth, product formation, and substrate utilization when multiple substrates are present and they are utilized in a sequential or simultaneous manner (data not shown). Thus, structure was added to the model to account for the intrinsic regulation of the cell in prioritization of substrates as well as in prioritization of growth and product formation. The structured model was able to capture the metabolic choices made by the organism in a complex medium. The model correctly predicted the differences in the substrate uptake kinetics on variation in the individual concentrations in the media. The optimal model strategy invoked for predicting the growth and product formation on the medium included simultaneous or sequential utilization of individual components. The choice of simultaneous or sequential utilization was dependent on the initial concentration present in the complex media. The model provided accurate estimation of overall growth and product formation rates as well as the individual substrate uptake rates. Such predictions will be useful in model based optimization and control.

The model development involves estimation of a number of parameters based on the growth on individual substrate combinations. Further, the initial metabolic state of the culture needs to be specified in the form of initial key enzyme concentrations. This initial state is dependent on pre-culturing conditions. It may be noted that the experiments presented here been conducted with a specific pre-culturing condition involving mainly free amino acids, peptides and proteins. A different pre-culture condition would change the initial metabolic state resulting in a different dynamic profile.

The model development methodology presented here can be applied to other industrially relevant fermentations. It would be of interest to verify the applicability of current model in: (i) model based optimization, (ii) inferential measurements, and (iii) pre-culture optimization.

NOMENCLATURE

μ_k^{max}: specific growth rate on substrate combination k
$q_{P,k}^{max}$: specific product formation rate on substrate combination k
S_1: free amino acids
S_2: glucose
S_3: ammonium sulfate
S_4: insoluble portion of Soya-CSL
N_T: total soluble nitrogen concentration
e_k: concentration of the enzyme responsible for uptake of substrate combination k
α_k: control parameter that determines the metabolic flux through branch k
β_k: degradation constant for the enzyme k

We thank Prof. Heinz Floss (Washington university, USA) for providing rifamycin B producing strain Amycolatopsis mediterranei S699, Lupin Pharma Ltd. (India) for providing rifamycin B and rifamycin O standards, and Regional Sophisticated Instrument Centre (RSIC) of Indian Institute of Technology, Mumbai for CHN analysis.

References

Bajpai-Dikshit J, Suresh AK, Venkatesh KV. 2003. An optimal model for representing the kinetics of growth and product formation by Lactobacillus rhamnosus on multiple substrates. J Biosci Bioeng 96(5):481–486.

Bally M, Egli T. 1996. Dynamics of substrate consumption and enzyme synthesis in Chelatobacter heintzii during growth in carbon-limited continuous culture with different mixtures of glucose and nitrilotriacetate. Appl Environ Microbiol 62(1):133–140.

ban Impe JF, Bastin G. 1995. Optimal adaptive control of fed-batch fermentation processes. Control Eng Pract 3(7):939–954.

Bapat PM, Wangikar PP. 2004. Optimization of Rifamycin B fermentation in shake flasks via a machine-learning-based approach. Biotechnol Bioeng 86(2):201–208.

Bapat PM, Kundu S, Wangikar PP. 2003. An optimized method for Aspergillus niger spore production on natural carrier substrates. Biotechnol Prog 19(6):1683–1688.

Basu A, Dixit SS, Phale PS. 2003. Metabolism of benzyl alcohol via catechol ortho-pathway in methylnaphthalene-degrading Pseudomonas putida CSV86. Appl Microbiol Biotechnol 62(5–6):579–585.

Benko PV, Wood TC, Segel IH. 1969. Multiplicity and regulation of amino acid transport in Penicillum chrysogenum. Arch Biochem Biophys 129:498–508.

Birol I, Undey C, Birol G, Cinar A. 2001. A web-based simulator for penicillin production. Int J Eng Simulation 2(1):24–30.

Calam CT. 1987. Process development in antibiotic fermentations. Cambridge: University of Cambridge. pp 1–217.

Cohen G, Shiffman D, Mevarech M, Aharonowitz Y. 1990. Microbial isopenicillin N synthase genes: Structure, function, diversity and evolution. Tr Biotech 8:105–111.

Daae EB, Ison AP. 1998. A simple structured model describing the growth of Streptomyces lividans. Biotechnol Bioeng 58(2–3):263–266.

Doshi P, Venkatesh KV. 1998. An optimal model for microbial growth in a multiple substrate environment: Simultaneous and sequential utilization. Process Biochem 33(6):663–670.

Doshi P, Rengaswamy R, Venkatesh KV. 1997. Modelling of microbial growth for sequential utilization in a multisubstrate environment. Process Biochem 32(8):643–650.

Emblay TM. 1991. The family Pseudonocardiaceae. In: Balows A, Truper HG, Dworkin M, Harder W, Schieifer KH, editors. The prokaryotes. New York: Springer Verlag. pp 996–1027.

Euverink GJW. 1995. Aromatic amino acid biosynthesis in actinomycetes. Groningen: University of Groningen.

Gygax D, Christ M, Ghisalba O, Nuesch J. 1982. Regulation of 3-deoxy-arabinoheptulosonic acid 7-phosphate synthetase in Nocardia mediterranei. FEMS Microbiol Lett 15(3):169–173.

Herrnstein RJ. 1974. Formal properties of the matching law. J Exp Ana Behav 21:15–164.

Kim CG, Kirschning A, Bergon P, Zhou P, Su E, Sauerbrei B, Ning S, Ahn Y, Breuer M, Leistner E, Floss HG. 1996. Biosynthesis of 3-amino-5-hydroxybenzoic acid, the precursor of mC(7)N units in ansamycin antibiotics. J Am Chem Soc 118(32):7486–7491.

Komives C, Parker RS. 2003. Bioreactor state estimation and control. Curr Opin Biotechnol 14(5):468–474.

Kompala DS, Ramakrishna D, Tsao GT. 1984. Cybernatic modelling of microbial growth in simple substrates. Biotechnol Bioeng 26:1272–1281.

Lendenmann U, Egli T. 1998. Kinetic models for the growth of Escherichia coli with mixtures of sugars under carbon-limited conditions. Biotechnol Bioeng 59(1):99–107.

Moore S. 1968. Amino acid analysis: Aqueous dimethyl sulfoxide as solvent for the ninhydrin reaction. J Biol Chem 243(23):6281–6283.

Narang A, Konopka A, Ramkrishna D. 1997. Dynamic analysis of the cybernetic model for diauxic growth. Chem Eng Sci 52(15):2567–2578.

Nielsen J, Villadsen J. 1994. Bioreaction engineering principles. New York: Plenum Press.

Pasqualucci CRVA, Radaelli P, Gallo GG. 1970. Improved differential spectrophotometric determination of rifamycins. J Pharm Sci 59:685–687.

Prabhu Y, Phale PS. 2003. Biodegradation of phenanthrene by Psuedomonas sp strain PP2: novel metabolic pathway, role of biosurfactant and cell surface hydrophobicity in hydrocarbon assimilation. Appl Microbiol Biotechnol 61(4):342–351.

Ramakrishna R, Ramkrishna D, Konopka AE. 1997. Microbial growth on substitutable substrates: Characterizing the consumer-resource relationship. Biotechnol Bioeng 54(1):77–90.

Ramkrishna D. 1982. A cybernetic perspective of microbial growth. In: Blanch HW et al., eds. Foundations of biochemical engineering, kinetics, and thermodynamics in biological systems. ACS Symposium Series 207:161–178.

Richard WJ, Lancini G. 1975. Production of Rifamycin B. USA. US Patent No. 3871965.

Van Dedem G, Moo-Young M. 1975. A model for diauxic growth. Biotechnol Bioeng 17:1301–1312.

Venkatesh KV, Doshi P, Rengaswamy R. 1997. An optimal strategy to model microbial growth in a multiple substrate environment. Biotechnol Bioeng 56(6):635–644.

Yu TW, Muller R, Muller M, Zhang XH, Draeger G, Kim CG, Leistner E, Floss HG. 2001. Mutational analysis and reconstituted expression of the biosynthetic genes involved in the formation of 3-amino-5-hydroxybenzoic acid, the starter unit of rifamycin biosynthesis in Amycolatopsis mediterranei S699. J Biol Chem 276(16):12546–12555.